3. Murray, C. A. in *Bond-Orientational Order in Condensed Matter Systems* (ed. Strandburg, K. J.) Ch. 4 (Springer, New York, 1992).
4. Fisher, D. S., Halperin, B. I. & Morf, R. Defects in the two-dimensional electron solid and implications for melting. *Phys. Rev. B* **20,** 4692–4712 (1979).
5. Cockayne, E. & Elser, V. Energetics of point defects in the two-dimensional Wigner crystal. *Phys. Rev. B* **43,** 623–629 (1991).
6. Frey, E., Nelson, D. R. & Fisher, D. S. Interstitials, vacancies, and supersolid order in vortex crystals. *Phys. Rev. B* **49,** 9723–9745 (1994).
7. Jain, S. & Nelson, D. R. Statistical mechanics of vacancy and interstitial strings in hexagonal columnar crystals. *Phys. Rev. E* **61,** 1599–1615 (2000).
8. Ashkin, A., Dziedzic, J. M., Bjorkholm, J. E. & Chu, S. Observation of a single-beam gradient force optical trap for dielectric particles. *Opt. Lett.* **11,** 288–290 (1986).
9. Crocker, J. C. & Grier, D. G. Methods of digital video microscopy for colloidal studies. *J. Colloid Interf. Sci.* **179,** 298–310 (1996).

Supplementary information is available on *Nature*'s World-Wide Web site (http://www.nature.com) or as paper copy from the London editorial office of *Nature*.

Acknowledgements

We thank S.C. Ying and D.A. Weitz for discussions. This work was supported by the National Science Foundation, the Petroleum Research Fund, and the Research Corporation. X.S.L. acknowledges the support of the A.P. Sloan Foundation.

Correspondence and requests for materials should be addressed to A.P. (e-mail: pertsin@barus.physics.brown.edu).

Evolution of magma-poor continental margins from rifting to seafloor spreading

R. B. Whitmarsh*, G. Manatschal† & T. A. Minshull*

* *Southampton Oceanography Centre, European Way, Southampton, SO14 3ZH, UK*
† *CGS-EOST, Université Louis Pasteur, 1 rue Blessig, 67084 Strasbourg, France*

The rifting of continents involves faulting (tectonism) and magmatism, which reflect the strain-rate and temperature dependent processes of solid–state deformation and decompression melting within the Earth[1,2]. Most models of this rifting have treated tectonism and magmatism separately, and few numerical simulations have attempted to include continental break-up and melting, let alone describe how continental rifting evolves into seafloor spreading. Models of this evolution conventionally juxtapose continental and oceanic crust. Here we present observations that support the existence of a zone of exhumed continental mantle, several tens of kilometres wide, between oceanic and continental crust on continental margins where magma-poor rifting has taken place. We present geophysical and geological observations from the west Iberia margin[3–7], and geological mapping of margins of the former Tethys ocean now exposed in the Alps[8–13]. We use these complementary findings to propose a conceptual model that focuses on the final stage of continental extension and break-up, and the creation of a zone of exhumed continental mantle that evolves oceanward into seafloor spreading. We conclude that the evolving stress and thermal fields are constrained by a rising and narrowing ridge of asthenospheric mantle, and that magmatism and rates of extension systematically increase oceanward.

The west Iberia–Newfoundland conjugate margins experienced a final Early Cretaceous phase of rifting and seafloor spreading that started ~133 Myr ago[7]. The Alpine Tethyan margins experienced a final Late Triassic/Early Jurassic rift phase presaging the Liguria–Piemonte ocean where seafloor-spreading magmatism began 160–165 Myr ago[13]. Both the west Iberia and Alpine magma-poor margins are characterized by margin-parallel deep-water zones, apparently representing successive stages of margin evolution, that is, thinned continental crust dissected by low-angle detachment faults succeeded by exhumed sub-continental mantle, with oceanward-increasing mafic melt volumes, that merges into oceanic crust[3,6,13,14]. We describe each zone in turn, adducing evidence from margins in both areas, before presenting models to explain the observations.

The west Iberia margin exhibits tilted fault blocks bounded by west-facing normal faults[5,14,15]. Under the slope and rise larger blocks lie 10–20 km apart over continental crust 20–30 km thick. Oceanward, wherever crustal blocks are $\lesssim$7 km thick, such faults are clearly listric (downward-flattening and concave upward), even penetrating the mantle, and closer together; the crust tapers oceanward to zero thickness within a distance of 50 km (Figs 1d and 2)[3–5,15,16]. Such blocks, where drilled by the Ocean Drilling Program (ODP), are capped by late Tithonian (~146 Myr ago) shallow-water sediments and therefore are continental crust[7]. Thus a marked change occurs in the mechanical response of the continental lithosphere to extension once the crust has been thinned to less than about 7 km.

In the southern Iberia abyssal plain (SIAP) three adjacent ODP boreholes (Sites 900, 1067 and 1068; Figs 1c and 2), near where the crust tapers to zero, yielded gabbro, amphibolite, tonalite gneiss, anorthosite (all part of a <400-m-thick basement layer floored by a sub-horizontal tectonic crust/mantle contact[16]) and serpentinized peridotite. The basement appears to be capped by a younger low-angle detachment fault that breaks out 6 km to the east and plunges into basement 14 km to the west[10]. The layer contains pre-rift lower crustal rocks, underplated in Late/post-Hercynian time (270 ± 3 ($\pm 1\sigma$) Myr ago), that later underwent ductile deformation (at 0.6–0.8 MPa) and cooling before exhumation at the seabed (<137 Myr ago)[10].

In the Alps, the continental crust of the distal Adria margin appears as fault blocks and as isolated allochthons (masses of rock that have been tectonically moved from their places of origin) separated by sub-horizontal detachments from underlying mantle[11]. This crust is mainly composed of Late to post-Hercynian granites intrusive into poly-metamorphic basement. Sporadically, underplated meta-gabbros exhumed from a pre-rift lower crustal level are observed which intruded the crust–mantle boundary during Late/post-Hercynian time[17]. Pressure–temperature–time (P–T–t) data indicate that the crust–mantle boundary was rather cool (~550 °C, 0.9–1.0 MPa) at the onset of rifting[18]. All structures genetically linked to the final phase of crustal extension, leading to formation of the zone of exhumed continental mantle (ZECM), are brittle structures.

Thus, the distal continental parts of the margins are dissected by listric detachment faults which either separate continental crustal blocks from mantle or occasionally penetrate the mantle. Where pre-rift lower crustal rocks are exhumed they frequently show mafic compositions and similar pre-rift P–T–t evolutions beginning with crustal underplating followed by isobaric cooling to 550 °C. Syn-rift melt products (contemporaneous with the rifting process) are absent. We estimate that durations of continental extension were, respectively, a few tens of Myr (at <5 mm yr^{-1}) for the Tethyan margins[19] and ~10 Myr (final phase, at >3.5 mm yr^{-1}) off Iberia[20].

The ZECM in the SIAP is 40- to 170-km wide with distinctive geophysical characteristics[3,4]. Morphologically, the basement surface identified on seismic reflection profiles may be divided into two regions of N–S-trending basement ridges and deep (~9 km) relatively low-relief basement (Fig. 1a and c); both narrow northward. Highly serpentinized peridotite was cored at four ODP sites mostly near the margins of the ZECM[7,21,22]. Primary-phase chemistry and clinopyroxene trace-element compositions indicate heterogeneous mantle depleted by heterogeneous, less than 10%,

partial melting, and percolated by mafic melts[21]. Trace-element compositions are more like sub-continental or suprasubduction-zone mantle than abyssal (oceanic) mantle[21,22]. Serpentinization began, at least locally, before seabed exhumation of the peridotite[23].

The SIAP ZECM has a seismic velocity structure which differs from those of the adjacent stretched continental and oceanic crusts (Fig. 1d)[3]. A 2–4-km-thick upper basement layer with a P-wave velocity of 4.5–7.0 km s^{-1} and a high velocity gradient (~1 s^{-1}) merges into a lower layer not more than 4 km thick with velocities of ~7.6 km s^{-1} and a low velocity gradient (<0.2 s^{-1}). Moho reflections are weak or absent. The top-basement velocity is lower than that of the adjacent continental crust, and the velocity in the lower layer is too high to represent magmatically intruded or underplated continental crust or even oceanic layer 3 (the lower oceanic crust)[3]. Therefore the velocity structure probably reflects decreasing mantle serpentinization with depth[3–5]. Low-amplitude N–S magnetic anomalies (Fig. 1a, c and e) indicate that ZECM basement magnetizations are typically much lower than those of oceanic basement further west, and the spectral properties of the anomalies suggest that most source bodies, equated here with syn-rift mafic intrusions (for example, ref. 24), lie not at top basement but up to 6.5 km deeper[6]. These observations suggest that the upper seismic layer contains little magmatic material, whereas the lower layer contains isolated N–S elongated magmatic intrusions which increase in volume oceanward (Fig. 1d). Although numerical models predict the addition of 3–5 km of melt to the ZECM we infer that, because the region of asthenospheric upwelling was relatively wide at this stage, very little decompression melting took place until the mantle viscosity structure approached that inferred to exist under a mid-ocean ridge[20].

In the Alps the sub-continental affiliation of mantle rocks is indicated by clinopyroxene Sr and Nd isotope compositions similar to many western Mediterranean sub-continental orogenic spinel lherzolites[25], by association with lower continental crust[26] and by isolated continental allochthons overlying exhumed mantle[12]. Sedimentary infill structures and serpentine clasts in post-rift Upper Jurassic deep-sea sediments indicate submarine exhumation. Deeper mantle rocks are encountered oceanwards. At the Platta nappe (sheet of rock thrust sideways over adjacent strata), gabbros 160.9 ± 0.5 Myr old were intruded into an already serpentinized peridotite[13] and provide direct evidence of syn-tectonic ZECM magmatism. Intrusion was immediately followed by emplacement of massive mid-ocean ridge basalt (MORB) pillows marking the onset of seafloor spreading[13].

Off Iberia, low-angle intrabasement ZECM faults have not been detected and deeply penetrating landward-dipping high-angle faults are imaged only rarely[5]. In contrast, Alpine geology, supported by top-basement tectono-sedimentary breccias in several ODP boreholes[7], reveals that the basement surface often represents the footwall of a series of mantle detachment faults individually accommodating ~10–20 km offsets in which the hanging wall moved oceanward. Because the faults cap basement highs that have minor submarine relief, despite their large offset, and enlisting

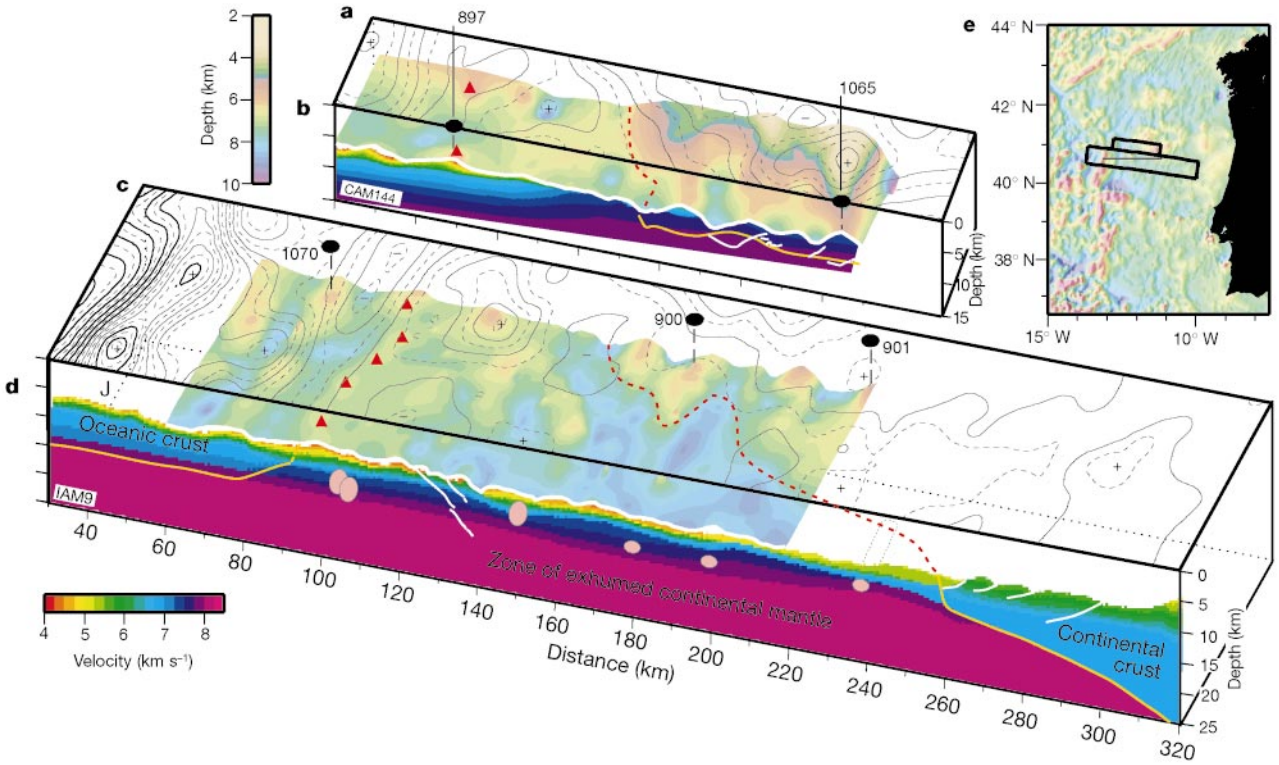

Figure 1 Exploded block diagram of the continental margin beneath the SIAP off west Iberia. **b**, **d**, Cross-sections of seismic profiles CAM144 (**b**, ref. 4) and IAM9 (**d**, ref. 3) colour-coded in km s^{-1} with the crust–mantle boundary in yellow-brown (where resolvable). **a**, **c**, Plan views of the three margin-parallel regions of thinned continental crust (bounded by dashed red line), the zone of exhumed continental mantle (ZECM) and the oceanic crust (roughly bounded by peridotite ridge, red triangles)[7]. The plan views also include relief of acoustic basement (depth below sea-level), contoured sea-surface magnetic anomalies (25 nT contours; crosses and dashes denote respectively peaks and troughs)[7,16] and ODP Sites 1070, 897, 900, 1065 and 901 (dots). Detachment faults (**b**; CAM144 thin white lines[16]) evolved as in Fig. 2, other deep faults in the ZECM (**d**; IAM9 white lines[5]) are suspected to be originally sub-horizontal mantle boundaries (Fig. 3c). The southern block illustrates how gabbroic margin-parallel magnetic source bodies (pink ellipses in **d**)—intruded within the ZECM and inferred to exist from magnetic anomaly inversions[6]—become more prevalent and closely spaced oceanwards, evolving eventually into a continuous layer of intrusions characteristic of ocean layer 3. **e**, Block locations, Lusigal-12 track (Fig. 2) and shaded-relief sea-surface magnetic anomalies.

other arguments (see Fig. 2b legend; ref. 10), we suggest that mantle exhumation was accomplished by concave-downward faults shortly before the onset of seafloor spreading.

Off west Iberia the ZECM merges into the earliest oceanic crust near a margin-parallel basement peridotite ridge[14] (Fig. 1d). High-amplitude linear margin-parallel magnetic anomalies immediately west of the peridotite ridge in the SIAP are consistent with seafloor spreading at 10 mm yr^{-1}, beginning around 126 Myr ago[27]. The seismic velocity structure gradually changes oceanwards to typically oceanic 10–20 km west of the peridotite ridge[3]. At ODP Site 1070, 20 km (representing ~2 Myr of spreading) oceanward of the peridotite ridge (Fig. 1d), we cored Late Aptian (112.2–116.9 Myr ago) sediments over pegmatite gabbro and depleted subcontinental serpentinized peridotite with gabbro veins[21,22] without encountering basaltic rocks. The gabbro had an enriched mid-ocean-ridge basalt (E-MORB) source[21]. The pegmatite cooled below 500 °C at 119 ± 0.7 Myr ago[10]. Thus, although near Site 1070 we encounter geophysical characteristics of normal oceanic crust, the cores reveal subcontinental mantle that was intruded by MORB dykes, exhumed at the seafloor and then sedimented shortly afterwards. The dates imply that tectonism of the earliest 'oceanic' crust continued after its emplacement over a region tens of kilometres wide.

In the Alps, oceanic crust is represented by undeformed MORB pillow lavas that thicken oceanwards. Generally, just oceanward of the edge of the continental crust, basalts form isolated bodies less

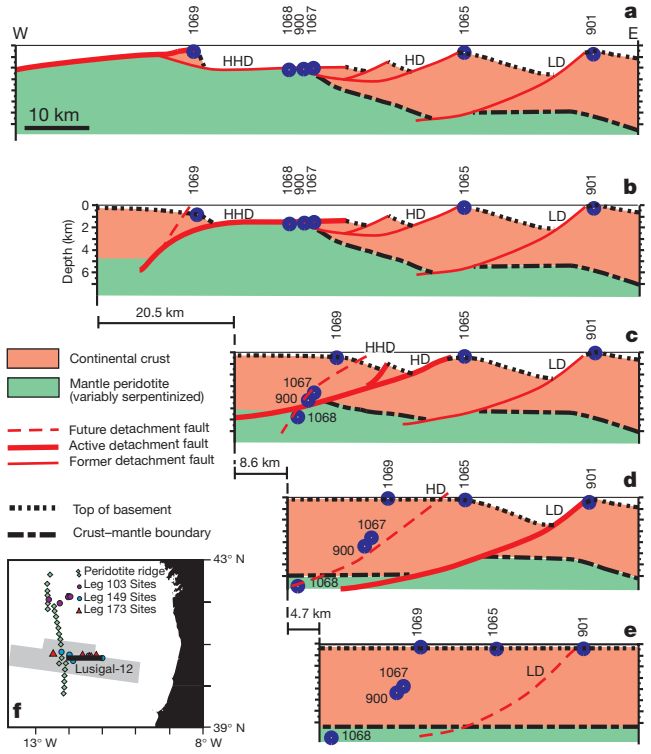

Figure 2 Palinspastic reconstruction with arbitrary reference datum[10] of profile Lusigal 12 (ref. 16) across the southern Iberia abyssal plain (SIAP). **a**, Tectonic interpretation of the depth-migrated multichannel seismic reflection profile. The total extension accommodated by the detachment faults LD, HD and HHD is around 34 km and this occurred between late Tithonian time and 137 Myr ago (that is, over a period of ≤9 Myr) at >3.5 mm yr^{-1}. Exhumation of about 75 km of subcontinental mantle within the ZECM at not less than 7.2 mm yr^{-1} was mainly accommodated by concave-downward faults[10]. **b**, Situation after mantle exhumation along the detachment HHD. The roll-over of HHD can explain three characteristic features: (1) the large (20.5 km) offset on this fault resulting in the observed minor submarine relief within most of the ZECM; (2) exhumation of subcontinental mantle by pulling it out from underneath a relatively stable hanging wall; and (3) the formation of tectono-sedimentary breccias on two basement highs drilled by the ODP (Sites 899 and 900/1067/1068) by a conveyor-belt-type sediment accumulation whereby the exhumed footwall rocks were fractured, exposed, and redeposited along the same active fault system. **c**, Situation at the onset of HHD and after motion on detachment HD stopped. We note the positions of Sites 900 and 1067 in the footwall of the later HHD; identical plagioclase ^{40}Ar/^{39}Ar ages (137 Myr ago) at both sites demonstrate that they cooled and were exhumed at the sea floor simultaneously. Thus, the transition from Fig. 2c to b had to occur about 137 Myr ago. **d**, Situation after extension along the detachment LD. We note the listric geometry of this fault, the relatively small 4.7 km offset along it, compared to the later detachment HHD, and its extension into brittle mantle. **e**, Situation at the onset of detachment faulting when continental crust was already thinned over a broad region by symmetric lithospheric-scale pure shear from about 30–35 km to about 7 km, showing distribution of the rocks eventually drilled by ODP. **f**, Track of profile Lusigal 12 and areas of Fig. 1 blocks.

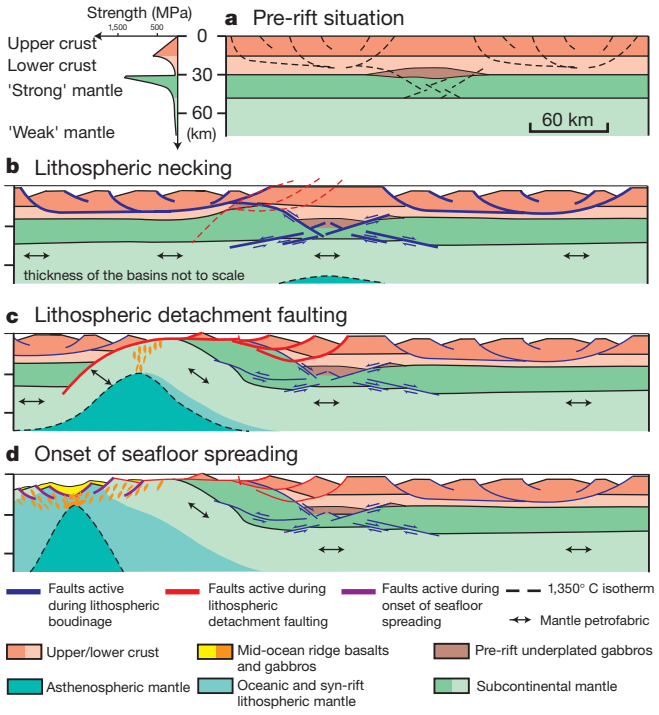

Figure 3 Conceptual lithosphere-scale model of development of a rifted magma-poor margin relative to a fixed right-hand edge. **a**, Initial situation with four-layer rheology (justified because the pre-rift lower crust often contains quartz-rich horizons[7,26]) and crust locally thickened by pre-rift underplated gabbro. **b**, Initially the upper mantle, the strongest part of the lithosphere, necked beneath the gabbros where it was weakest, allowing the asthenosphere to rise. Elsewhere, ductile flow of the lower crust determined where rift basins formed at the surface. Relatively little crustal thinning and subsidence occurred above the necked region, whereas the adjacent areas were strongly thinned. Arrows indicate a hypothetical, initially sub-horizontal, petrofabric. **c**, Later, the thermal structure and gravitational response associated with the rising asthenosphere started to influence the rifting. Then, rifting was localized at the margin of the relatively weak unextended, or only slightly extended, crust. This allows the important initial thinning of the lower crust and its observed abrupt transition to weakly thinned crust (see for example refs 17 and 26) to be explained. The change in extensional geometry from listric to one or more concave-downward faults reflected a change in the distribution of weak layers. Whereas listric faults sole out in horizontal weak layers, concave-downward faults might be favoured by sub-vertical weak zones, possibly resulting from rising magma and higher thermal gradients above the rising and narrowing asthenosphere. **d**, The asthenosphere ascended close to the surface and mid-ocean-ridge basalt melts were intruded into, and even extruded onto, sub-continental mantle. Deeper mantle layers were exhumed oceanward. Eventually, increasing melt production led to the creation of 'continuous' oceanic crust and the asthenosphere spawned oceanic upper mantle. Seafloor spreading had begun.

than 100 m thick; further oceanwards, basalt bodies are aligned parallel to the margin. The first voluminous basalts show a clearly MORB isotopic signature[13] and overlie tectonically exhumed sub-continental mantle.

Thus, generally, after the break-up of continental crust, mafic intrusives and/or extrusives increase in volume oceanwards across the ZECM. They have a MORB signature, yet intrude and overlie sub-continental mantle. Eventually, such a 'crust' can acquire a geophysically oceanic signature possibly even before extrusives/intrusives of oceanic layer 2 (upper oceanic crust) are widespread.

We now explain how the upper ~7 km of the ZECM evolves into oceanic crust formed by seafloor spreading, before we present a broader lithospheric-scale perspective. In a late stage of rifting, when the continental crust was already locally thinned to about 7 km (Fig. 2e), extension became focused within the future distal margin and was accommodated by detachment faulting (Fig. 2d to b). Exhumation of sub-continental mantle was mainly accommodated by concave-downward faults (Fig. 2b to a). The crust and uppermost mantle underwent brittle deformation and extension was dominated by simple shear. Seafloor spreading, heralded by an oceanward-increasing emplacement of MORB melt over, and into, depleted sub-continental mantle, eventually generated a thin oceanic crust (Fig. 1d). Tectonism remained active over a broad zone at least until slow seafloor-spreading had started. Extension rates increased by factors of 2–3 from the latest continental rifting to the earliest seafloor spreading.

Our conceptual lithospheric-scale model (Fig. 3) exhibits the well known sequential modes of extension from pure shear to simple shear to slow seafloor-spreading. However, only now can we characterize the simple-shear phase, infer its 'genetic' link to the preceding pure-shear phase and understand its link to the subsequent seafloor-spreading phase. Rifting began with an isostatically equilibrated ~30-km-thick continental crust (Fig. 3a). Initial rifting was controlled by ductile flow of the lower crust, as suggested by some numerical models[28], and associated with subsidence[9]. Rift basins were bounded by listric faults that levelled out at mid-crustal levels, where the crust was weaker, and decoupled upper crust and upper mantle deformation. Rifting was distributed over the entire future margin (Fig. 3b). The extending crust cooled during ongoing rifting. Magmatism was essentially absent during this initial stage of rifting and the rift was, on a lithospheric scale, symmetric.

Mechanically or thermally induced weaknesses in the upper mantle, possibly resulting from pre-rift underplating, controlled the initial location of upper mantle necking which can be offset from crustal deformation, as in some numerical models (see, for example, ref. 28). The weaknesses guided the ascent of the asthenosphere, which in turn controlled the location and evolution of the latest rifting and eventual continental break-up (Fig. 3c). The transition from symmetric non-magmatic rifting to seafloor spreading included a transient phase of simple-shear dominated, and partly asymmetric, continental rifting that coincided with the onset of systematically increasing magmatism. This transition was characterized by the localization of extension along continental crust and even upper mantle detachment faults and then along top-to-the-ocean and concave-downward faults, leading to the exhumation of the ZECM (Fig. 3c). Finally, the ascending but narrowing asthenospheric mantle (Fig. 3d) led to the typical focused magmatism and tectonism of a mid-ocean ridge.

Although our model involves mechanisms of tectonic deformation that are not yet fully understood or proved, it does explain a wide range of observations. It predicts low-angle detachments in continental crust (Fig. 2a), a systematic oceanward increase in syn-kinematic MORB extrusives/intrusives across the ZECM (Fig. 3d) and a systematic trend from shallow to deeper exhumed sub-continental mantle rocks across a reconstructed conjugate pair of ZECMs in association with a rotation of mantle rock structures (Fig. 3c).

Other authors have suggested that other magma-poor rifted margins in the North Atlantic[29] and elsewhere have characteristics, including ZECMs, that are at least partially similar to those presented above. Elsewhere, for example, in the Woodlark Basin[30], the transition from continent to ocean appears to be more abrupt. Further observations may resolve whether these differences result from differing rates and durations of extension and/or other factors. □

Received 19 March; accepted 19 July 2001.

1. McKenzie, D. P. & Bickle, M. J. The volume and composition of melt generated by extension of the lithosphere. *J. Petrol.* **29,** 625–679 (1988).
2. England, P. Constraints on extension of continental lithosphere. *J. Geophys. Res.* **88,** 1145–1152 (1983).
3. Dean, S. M., Minshull, T. A., Whitmarsh, R. B. & Louden, K. Deep structure of the ocean-continent transition in the southern Iberia Abyssal Plain from seismic refraction profiles: II The IAM-9 transect at 40° 20′ N. *J. Geophys. Res.* **105,** 5859–5886 (2000).
4. Chian, D., Louden, K. E., Minshull, T. A. & Whitmarsh, R. B. Deep structure of the ocean-continent transition in the southern Iberia Abyssal Plain from seismic refraction profiles: Ocean Drilling Program (Legs 149 and 173) transect. *J. Geophys. Res.* **104,** 7443–7462 (1999).
5. Pickup, S. L. B., Whitmarsh, R. B., Fowler, C. M. R. & Reston, T. J. Insight into the nature of the ocean-continent transition of West Iberia from a deep multichannel seismic reflection profile. *Geology* **24,** 1079–1082 (1996).
6. Whitmarsh, R. B. *et al.* in *Non-Volcanic Rifting of Continental Margins: A Comparison of Evidence from Land and Sea* (eds Wilson, R. C. L., Whitmarsh, R. B., Taylor, B. & Froitzheim, N.) 107–124 (Geological Society of London, London, in the press).
7. Whitmarsh, R. B. & Wallace, P. J. in *Proc. ODP Sci. Results* (eds Beslier, M. O., Whitmarsh, R. B., Wallace, P. J. & Girardeau, J.) 1–36 (Ocean Drilling Program, College Station, Texas, 2001).
8. Lagabrielle, Y. & Lemoine, M. Alpine, Corsican and Apennine ophiolites: the slow-spreading ridge model. *C. R. Acad. Sci. Ser. 2a* **325,** 909–920 (1997).
9. Manatschal, G. & Bernoulli, D. Architecture and tectonic evolution of nonvolcanic margins: present-day Galicia and ancient Adria. *Tectonics* **18,** 1099–1199 (1999).
10. Manatschal, G., Froitzheim, N., Rubenach, M. J. & Turrin, B. in *Non-Volcanic Rifting of Continental Margins: A Comparison of Evidence from Land and Sea* (eds Wilson, R. C. L., Whitmarsh, R. B., Taylor, B. & Froitzheim, N.) 405–428 (Geological Society of London, London, in the press).
11. Manatschal, G. & Nievergelt, P. A continent-ocean transition recorded in the Err and Platta nappes (Eastern Switzerland). *Eclogae Geol. Helvetiae* **90,** 3–27 (1997).
12. Froitzheim, N. & Manatschal, G. Kinematics of Jurassic rifting, mantle exhumation, and passive margin formation in the Austroalpine and Penninic nappes (eastern Switzerland). *Geol. Soc. Am. Bull.* **108,** 1120–1133 (1996).
13. Desmurs, L., Manatschal, G. & Bernoulli, D. in *Non-Volcanic Rifting of Continental Margins: A Comparison of Evidence from Land and Sea* (eds Wilson, R. C. L., Whitmarsh, R. B., Taylor, B. & Froitzheim, N.) 235–266 (Geological Society of London, London, in the press).
14. Boillot, G., Féraud, G., Recq, M. & Girardeau, J. Undercrusting by serpentinite beneath rifted margins. *Nature* **341,** 523–525 (1989).
15. Reston, T. J., Krawczyk, C. M. & Kläschen, D. The S reflector west of Galicia (Spain). Evidence for detachment faulting during continental breakup from prestack depth migration. *J. Geophys. Res.* **101,** 8075–8091 (1996).
16. Whitmarsh, R. B., Dean, S. M., Minshull, T. A. & Tompkins, M. Tectonic implications of exposure of lower continental crust beneath the Iberia Abyssal Plain, northeast Atlantic Ocean: geophysical evidence. *Tectonics* **19,** 919–942 (2000).
17. Hermann, J., Müntener, O., Trommsdorff, V., Hansmann, W. & Piccardo, G. B. Fossil crust-to-mantle transition, Val Malenco (Italian Alps). *J. Geophys. Res.* **102,** 20123–20132 (1997).
18. Müntener, O., Hermann, J. & Trommsdorff, V. Cooling history and exhumation of lower-crustal granulite and upper mantle (Malenco, eastern central Alps). *J. Petrol.* **41,** 175–200 (2000).
19. Bertotti, G., Picotti, V., Bernoulli, D. & Casterllarin, A. From rifting to drifting tectonic evolution of the South-Alpine upper crust from the Triassic to the Early Cretaceous. *Sedim. Geol.* **86,** 53–76 (1993).
20. Minshull, T. A., Dean, S. M., White, R. S. & Whitmarsh, R. B. in *Non-Volcanic Rifting of Continental Margins: A Comparison of Evidence from Land and Sea* (eds Wilson, R. C. L., Whitmarsh, R. B., Taylor, B & Froitzheim, N.) 537–550 (Geological Society of London, London, in the press).
21. Hébert, R., Gueddari, K., Laflèche, M. R., Beslier, M.-O. & Gardien, V. in *Non-Volcanic Rifting of Continental Margins: A Comparison of Evidence from Land and Sea* (eds Wilson, R. C. L., Whitmarsh, R. B., Taylor, B. & Froitzheim, N.) 161–189 (Geological Society of London, London, in the press).
22. Abe, N. in *Non-Volcanic Rifting of Continental Margins: A Comparison of Evidence from Land and Sea* (eds Wilson, R. C. L., Whitmarsh, R. B., Taylor, B. & Froitzheim, N.) 143–159 (Geological Society of London, London, in the press).
23. Skelton, A. D. L. & Valley, J. W. The relative timing of serpentinization and mantle exhumation at the ocean-continent transition, Iberia: constraints from oxygen isotopes. *Earth Planet. Sci. Lett.* **178,** 327–338 (2000).
24. Schärer, U., Girardeau, J., Cornen, G. & Boillot, G. 138–121 Ma asthenospheric magmatism prior to continental break-up in the North Atlantic and geodynamic implications. *Earth Planet. Sci. Lett.* **181,** 555–572 (2000).
25. Rampone, E. *et al.* Petrology, mineral and isotope geochemistry of the External Liguride peridotites (Northern Apennines, Italy). *J. Petrol.* **36,** 81–105 (1995).
26. Müntener, O. & Hermann, J. in *Non-Volcanic Rifting of Continental Margins: A Comparison of Evidence from Land and Sea* (eds Wilson, R. C. L., Whitmarsh, R. B., Taylor, B. & Froitzheim, N.) 267–288 (Geological Society of London, London, in the press).
27. Whitmarsh, R. B., Miles, P. R., Sibuet, J.-C. & Louvel, V. in *Proc. ODP Sci. Results* (eds Whitmarsh, R. B., Sawyer, D. S., Klaus, A. & Masson, D. G.) 665–674 (Ocean Drilling Program, College Station, Texas, 1996).

28. Harry, D. L. & Sawyer, D. S. A dynamic model of extension in the Baltimore Canyon Trough region. *Tectonics* **11,** 420–436 (1992).
29. Louden, K. E. & Chian, D. in *Response of the Earth's Lithosphere to Extension* (eds White, R. S., Hardman, R. F. P., Watts, A. B. & Whitmarsh, R. B.) 767–799 (Phil. Trans. R. Soc. Ser. A, Royal Society, London, 1999).
30. Taylor, B., Goodliffe, A. M. & Martinez, F. How continents break up: Insights from Papua New Guinea. *J. Geophys. Res.* **104,** 7497–7512 (1999).

Acknowledgements

We thank the Shipboard Scientific Parties of ODP Leg 149 and Leg 173 and those aboard RRS *Discovery* cruise 215. We thank the UK Natural Environment Research Council, The Royal Society of London and the Swiss National Science Foundation for support.

Correspondence and requests for materials should be addressed to R.B.W. (e-mail: rbw@soc.soton.ac.uk).

Mitochondrial protein phylogeny joins myriapods with chelicerates

Ui Wook Hwang*†, Markus Friedrich‡, Diethard Tautz§, Chan Jong Park† & Won Kim†

** Department of Biology, Teachers College, Kyungpook National University, Taegu 702-701, Korea*
† School of Biological Sciences, Seoul National University, Seoul 151-742, Korea
‡ Department of Biological Sciences, Wayne State University, 5047 Gullen Mall, Detroit, Michigan 48202, USA
§ Abteilung für Evolutionsgenetik, Institut für Genetik, Universität zu Köln, Weyertal 121, 50931 Köln, Germany

The animal phylum Arthropoda is very useful for the study of body plan evolution given its abundance of morphologically diverse species and our profound understanding of *Drosophila* development[1]. However, there is a lack of consistently resolved phylogenetic relationships between the four extant arthropod subphyla, Hexapoda, Myriapoda, Chelicerata and Crustacea. Recent molecular studies[2–4] have strongly supported a sister group relationship between Hexapoda and Crustacea, but have not resolved the phylogenetic position of Chelicerata and Myriapoda. Here we sequence the mitochondrial genome of the centipede species *Lithobius forficatus* and investigate its phylogenetic information content. Molecular phylogenetic analysis of conserved regions from the arthropod mitochondrial proteome yields highly resolved and congruent trees. We also find that a sister group relationship between Myriapoda and Chelicerata is strongly supported. We propose a model to explain the apparently parallel evolution of similar head morphologies in insects and myriapods.

The basal diversification of arthropod lineages, which date back into the late Cambrian period is still unclear. Morphological analyses[5,6] all suggest a monophyletic Arthropoda within which insects and myriapods are most closely related. Controversy, however, continued over whether insects, myriapods and crustaceans form a second major subclade, Mandibulata, on the basis of the shared derived possession of mandibles[5] or whether crustaceans are a sister group to chelicerates on the basis of the occurrence of biramous appendages in representatives of both groups[6]. Several independent molecular studies provided strong support for arthropod monophyly, a monophyletic Hexapoda, Myriapoda and Chelicerata, and, most significantly, a sister group relationship between insects and crustaceans (Pancrustacea) (for a review see ref. 7). Although they ruled out the possibility of insect/myriapod or crustacean/chelicerate sister clades, previous molecular studies did not resolve relationships between myriapods, chelicerates and Pancrustacea[2–4]. Mitochondrial gene order rearrangements were initially interpreted to support a monophyletic Mandibulata[8], but were later re-interpreted to further corroborate the Pancrustacea clade[2].

Complete mitochondrial genome sequences can be informative at deep phylogenetic levels[9]. We therefore investigated their potential use for arthropod phylogeny. As examples of mitochondrial genomes are known from all arthropod subphyla except myriapods, we determined the complete mitochondrial genome sequence of the centipede *Lithobius forficatus*. The *Lithobius* mitochondrial genome is 15,437 base pairs (bp) (details will be given elsewhere). Gene content and arrangement correspond to that of conservatively evolving arthropod mitochondrial genomes with two exceptions. Most crustacean and insect mitochondrial genomes differ from *Lithobius* with regard to the position of the transfer RNA$^{Leu(UUR)}$ gene, which in crustaceans is located between the COXI and COXII genes and in *Lithobius* between the tRNA$^{Leu(CUN)}$ and ND1 genes. This is consistent with the previous demonstration that the COXI/tRNA$^{Leu(UUR)}$/COXII arrangement is a synapomorphy of the Pancrustacea[2].

Another difference concerns the position of the tRNA^{Cys} gene, which in most arthropods resides between tRNA^{Trp} and tRNA^{Tyr} (Fig. 1), but in *Lithobius* it lies within the non-coding region of the

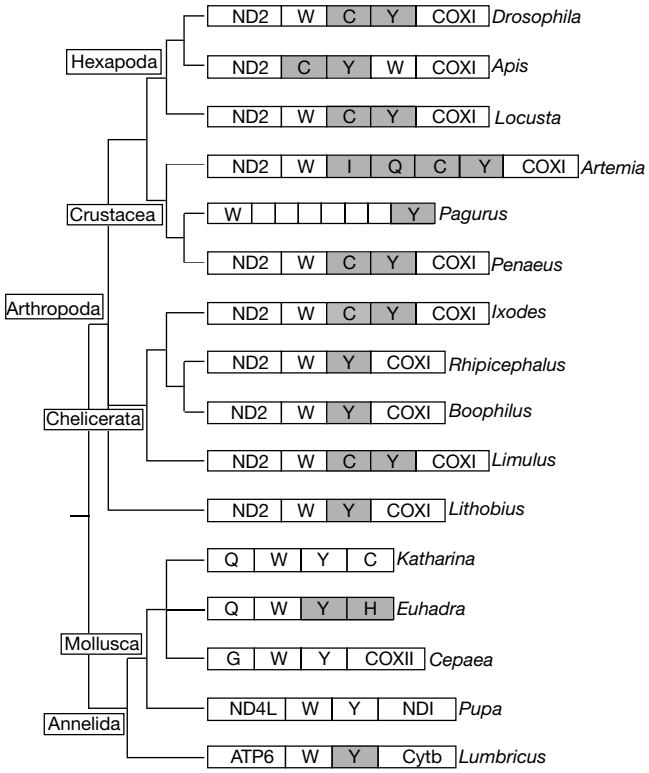

Figure 1 Phylogenetic distribution of tRNA^{Cys} arrangements in arthropod mitochondrial genomes. The relative location of tRNA^{Trp} (W), tRNA^{Cys} (C) and tRNA^{Tyr} (Y) is shown for representative arthropod and outgroup species with similar arrangements. Multiple coding units separating tRNA^{Trp} and tRNA^{Tyr} in *Pagurus* are indicated by boxes. Transcription units in clear boxes code from left to right, those in shaded boxes code from right to left. The mollusc *Euhadra herklotsi* is the only non-arthropod species known so far in which tRNA^{Trp} and tRNA^{Tyr} are neighbours in opposite coding orientation, as in *Lithobius*. In a few non-arthropod species tRNA^{Trp} and tRNA^{Tyr} are next to each other, although in the same coding orientation. Re-examining non-annotated regions in published mitochondrial genome sequences, we found that the annelid species *Lumbricus terrestris* has coding probability for a second tRNA^{Tyr}, which could result in a *Lithobius*-like tRNA^{Trp} and tRNA^{Tyr} arrangement (U.W.H., unpublished observation). This possibility, however, awaits confirmation by tRNA transcript analysis.